

# STATUS OF THE SWISSFEL C-BAND LINEAR ACCELERATOR

F. Loehl, J. Alex, H. Blumer, M. Bopp, H. Braun, A. Citterio, U. Ellenberger, H. Fitze, H. Joehri, T. Kleeb, L. Paly, J. Raguin, L. Schulz, R. Zennaro, Paul Scherrer Institut, Villigen PSI, Switzerland

## Abstract

This paper summarizes the status of the linear accelerator (linac) of the Swiss free-electron laser SwissFEL. The linac will be based on C-band technology and will use solid-state modulators and a novel type of C-band accelerating structures which has been designed at PSI. Initial test results of first 2 m long structures will be presented together with measurements performed with the first BOC-type pulse compressors. Furthermore, we will present first results of a water cooling system for the accelerating structures and the pulse compressors.

## INTRODUCTION

The SwissFEL [1] is an x-ray free-electron laser that is currently under construction at Paul Scherrer Institut in Switzerland. A schematic layout of the facility is depicted in Fig. 1. In an initial phase, the project includes the main accelerator and a hard x-ray line called Aramis. A soft x-ray line, Athos, can be added at a later stage. The facility will operate at a repetition rate of 100 Hz and uses an S-band photo-injector to generate an ultra-bright electron beam that is accelerated to a beam energy of about 380 MeV in S-band structures. After the first magnetic bunch compressor chicane, the beam enters the main linac, which is based on C-band technology. The linac is divided into three segments. Linac 1 accelerates the beam to an energy of 2.1 GeV after which the beam is compressed in a second magnetic bunch compressor chicane. Linac 2 boosts the energy to 3 GeV. At this point, a switch-yard will be installed to allow distributing two electron bunches that are accelerated within a single RF pulse - spaced by 28 ns in time - to Aramis and Athos. After this switch yard, linac 3 accelerates the beam to its maximum energy of 5.8 GeV. Finally, the beam enters an around 60 m long undulator in which x-ray radiation ranging from 0.1 to 0.7 nm is generated.

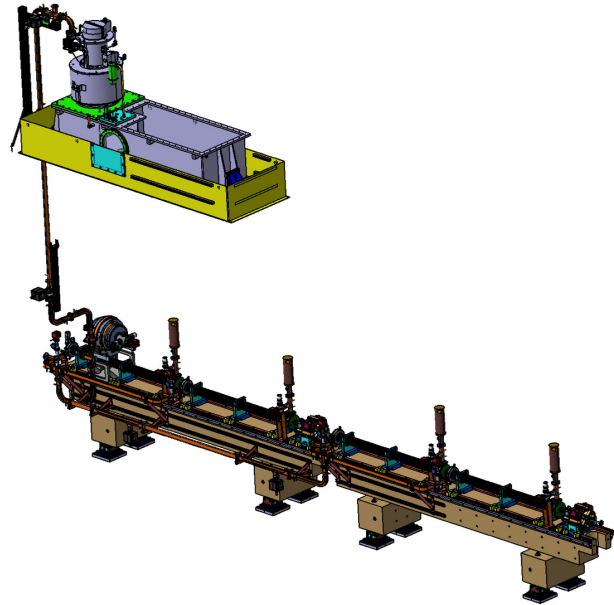


Figure 2: Layout of a linac module consisting out of the RF source (modulator not shown), the waveguide network, a BOC-type pulse compressor, and four 2 m long C-band structures.

## C-BAND LINAC MODULE

The C-band linac consists out of 26 linac modules each of which comprises an RF source, a waveguide network, a barrel-open cavity (BOC) type pulse compressor, and four 2 m long accelerating structures. A schematic of a linac module is shown in Fig. 2. The RF source is placed in the technical gallerie on top of the accelerator, shielded by a concrete ceiling of 1.5 m thickness. The accelerating structures and the RF pulse compressor are installed on two granite girders, and the design is made in such a way

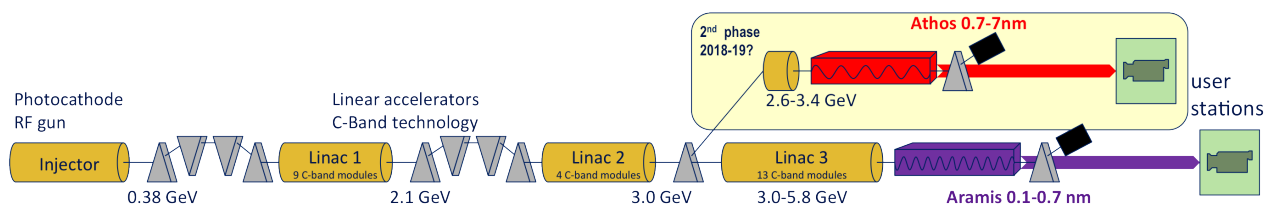


Figure 1: Schematic layout of the SwissFEL facility. It consists of an S-band injector, a C-band linear accelerator, and two undulator lines. The hard x-ray line Aramis will be built in the first project phase and in a second project phase the soft x-ray line Athos can be added.

that the girders can be pre-assembled outside of the accelerator tunnel to minimize installation times. At the end of the second girder and for some modules also at the end of the first girder, a beam position monitor and an air-cooled quadrupole magnet [2] is installed. Some modules include further diagnostics components such as screen monitors, wire scanners, or collimators.

## RF SOURCE

Toshiba klystrons of type E37212 will be used to generate RF pulses up to 50 MW of power with durations of  $3 \mu\text{s}$  at a 100 Hz rate. These klystrons allow operating the collector at a temperature of  $80^\circ\text{C}$ , which will be utilized at SwissFEL to recover part of the energy and utilize it to heat buildings on the PSI campus. The total power saving can be up to 9000 MWh/y. A first such klystron is successfully running in our test stand since spring this year.

The klystrons will be driven by solid-state modulators. In our test stand, we currently operate a ScandiNova K2 modulator. We ordered an improved prototype modulator from ScandiNova which will be further optimized and include a real-time control system. Furthermore, the stability of this new prototype modulator will be improved. PSI is in close contact to ScandiNova to support this development.

A second modulator prototype was ordered from a consortium of Ampegon and PPT. This second modulator will be based on the design of the so called Pulse Genesis modulator, which is developed by a collaboration of ABB, PPT, the ETH Zuerich, and PSI. This second modulator prototype is expected to be delivered to PSI mid-2014.

## WAVEGUIDE NETWORK

The fact that the waveguide network is attached directly to the girders - and this is required in order to allow for a pre-assembly of the girders - has the consequence that the mechanical tolerances of the waveguide network are more demanding. In order to minimize phase offsets between the four accelerating structures, we specify a tolerance of  $\pm 0.2 \text{ mm}$  in the length of the connecting waveguide segments. Currently, we are in the process of testing various waveguide components from different manufacturers. This includes water loads from CML and dry-loads from IHEP. Furthermore, we developed our own directional couplers, H-splitters, and E-splitter, which currently are finalized and are planned to be high-power tested later this year. The design for the directional coupler avoids feedthroughs to reduce costs and to allow for a baking. Furthermore, we designed and built a vacuum waveguide valve, which was finished recently and is also planned to be high power tested later this year.

## PULSE COMPRESSOR

The RF pulses from the klystron are compressed in a barrel-open-cavity type pulse compressor [3] (see [4] for further details). This pulse compressor was designed at PSI

and a first prototype was manufactured by VDL. Figure 3 shows a picture of this first pulse compressor. Since the beginning of this year, this pulse compressor is installed in our C-band test stand where it was successfully tested with RF pulses of up to 50 MW of power at the nominal pulse duration.

Figure 4 shows the RF pulse after the pulse compressor for two settings. In the first setting, a 50 MW pulse was sent into the pulse compressor and towards the end of the RF pulse, a  $180^\circ$  phase jump was applied. This yields an RF pulse at the output of the BOC with a peak power of

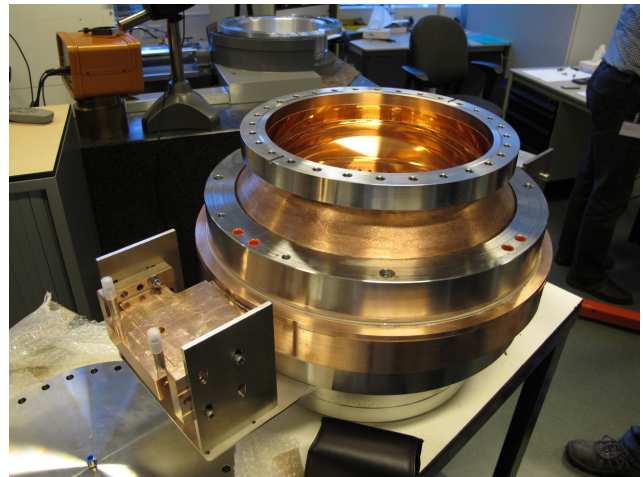


Figure 3: Image of the first BOC-type pulse compressor.

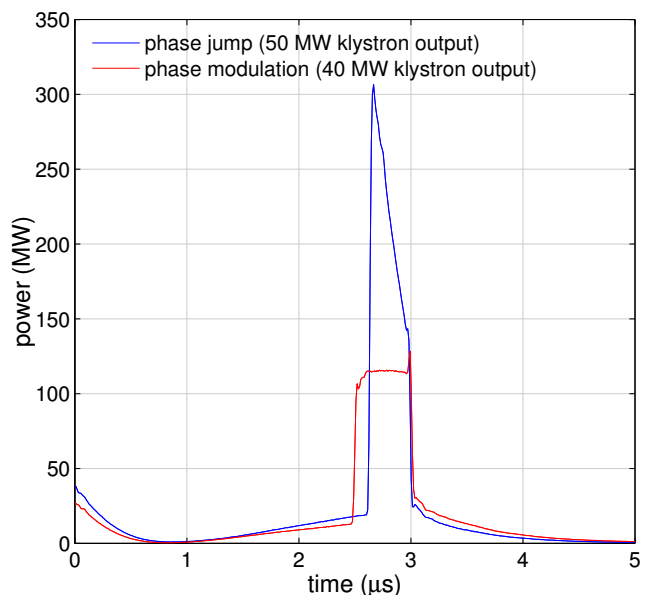


Figure 4: Two example RF pulses generated with the first BOC-type pulse compressor. Blue: generation of high-peak-power pulse by applying a 180 degree phase jump. Red: generation of a flat-top pulse by applying a proper feed-forward table for the RF phase.



Figure 5: First 2 m long PSI C-band structure after the brazing.

more than 300 MW. In the second example, a 40 MW input pulse was utilized and the phase of this pulse was temporally shaped in such a way that a flat-top pulse is generated at the output of the pulse compressor. For SwissFEL, this second approach is a considered mode of operation for linac 1 for the case that two or more pulses are accelerated within the same RF pulse. A flat-top will make it easier to achieve similar phase and amplitude settings for the individual bunches.

## ACCELERATING STRUCTURES

The 2 m long accelerating structures that will be utilized for the SwissFEL linac have been designed at PSI. After several initial test structures [5] of about 30 cm length, the first 2 m long accelerating structure was brazed at PSI in April this year. A picture of this first structure is shown in Fig. 5. Up to now, a total of three structures have been manufactured and more details can be found in ref. [6].

The first two structures were not vacuum tight after they were brazed but both of them could be repaired with a second brazing step. For the third structure, the amount of brazing alloy was increased by the same amount that was added during the repair of the first two structures. Furthermore, the brazing temperature was reduced. This third structure was vacuum tight after brazing and now RF measurements have to be performed to verify that the increased

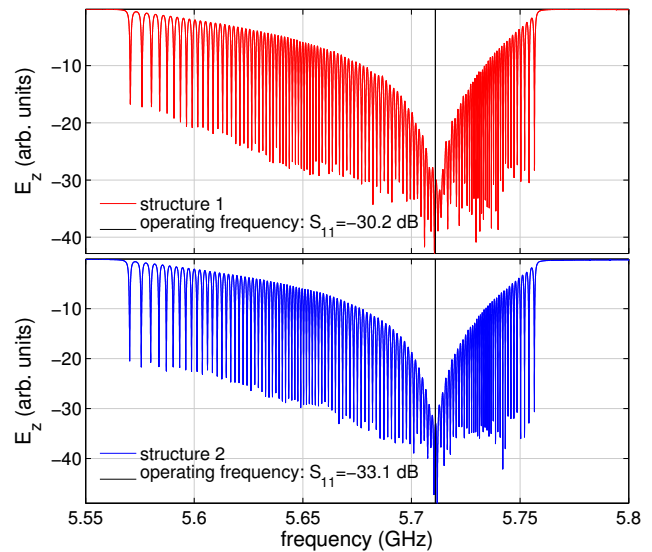


Figure 6: Measured reflection parameter  $S_{11}$  for the first two 2 m long PSI C-band structures.

amount of brazing alloy does not affect the RF properties.

The RF properties of the first two C-band structures have been measured using the bead-pull technique, and the results are summarized in Figs. 6 to 8. Both structures achieved an excellent reflection parameter  $S_{11}$  of -30.2 dB and -33.1 dB respectively (see Fig. 6). The electric field profile along the longitudinal coordinate of the structures is depicted in Fig. 7. There is only a very small standing wave contribution visible caused by a small reflection from the output coupler. This reflection was reduced from structure 1 to structure 2 by slight adjustments to the output-coupler dimensions. Figure 7 shows the computed errors in the phase advance for each cell. Also here, an improvement from structure 1 to structure 2 is visible, but both structures provide excellent phase advance errors of only around  $\pm 2^\circ$ .

The first structure is currently installed in the C-band test stand and tested under high RF load. Processing of the structure was very fast. It took only a few days to achieve nominal RF power within the structure - 10 MW, 3  $\mu$ s duration at the input of the pulse compressor resulting in  $\sim 28$  MV/m of accelerating gradient in the structure. Meanwhile, up to 28 MW of RF power have been applied to the structure, yielding an accelerating gradient of  $\sim 52$  MV/m, almost twice the nominal gradient.

Initial break-down measurements have been performed, giving a break-down rate of  $\sim 2.1 \times 10^{-6}$  at an accelerating gradient of 52 MV/m. When operated at the nominal gradient, this will result in an excellent break-down rate well below the anticipated goal of  $10^{-8}$ .

## TEMPERATURE CONTROL

A first prototype of a temperature stabilization unit has been tested. The system was utilized to control the temperature of the pulse compressor in the test stand, but a similar

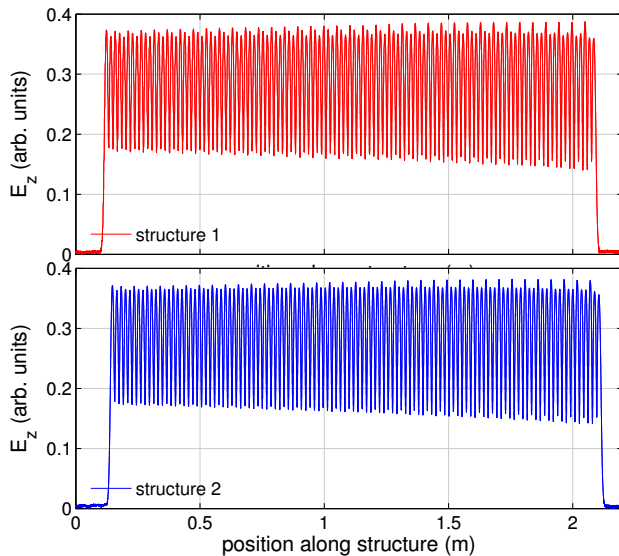


Figure 7: Measured electric field distribution along the longitudinal coordinate of the first two 2-m long PSI C-band structures.

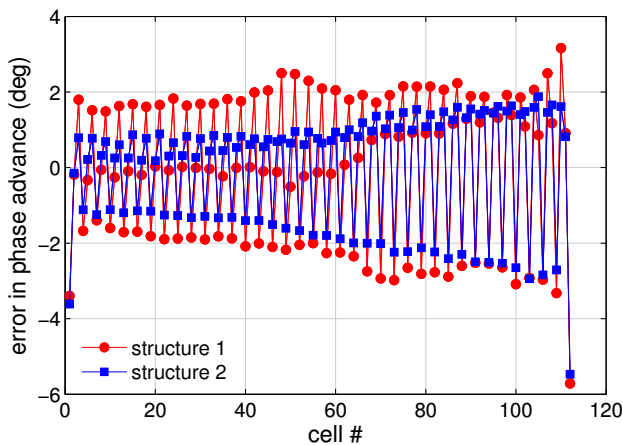


Figure 8: Errors in the phase advance of the 111 C-band cells of the first two 2-m long PSI C-band structures.

circuit is foreseen for the temperature control of the four accelerating structures. A schematic of the setup is shown in Fig. 9. The system consists of a water circuit into which cold water can be injected. The mixing ratio between the cold water from the supply line and the water circulating in the local circuit can be adjusted with an adjustable valve. A heater with a total power of 2.4 kW is installed within the local circuit and it is used to precisely control the water temperature at the inlet of the pulse compressor. In order to optimize the speed of the regulation a feed-forward algorithm is used to drive the heater. The required heater power is calculated from the difference between the desired temperature  $T_{SP}$  at sensor  $T_3$  and the temperature  $T_2$  before the heater. With this algorithm, the the temperature measured

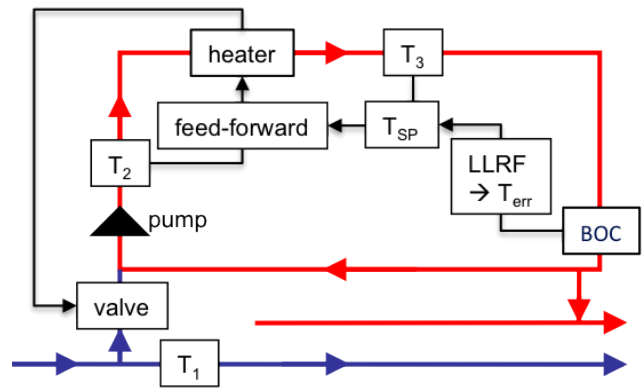


Figure 9: Simplified schematic of the prototype temperature stabilization system for the BOC-type pulse compressor.

at sensor  $T_3$  can be stabilized to a precision of 3 mK (rms), which is also the resolution limit of the temperature sensor.

Using low-level RF measurements, we are capable of measuring the error frequency of the pulse compressor with high precision. Since the required water temperature at the inlet of the pulse compressor changes with the RF power level, we implemented an additional control loop which adjusts  $T_{SP}$  of the main control loop based on low-level RF measurements. This makes sure that the water temperature is appropriately adjusted for varying RF power levels, and it also allows stabilizing the frequency at an adjustable frequency offset. The latter option is required, for example, when the pulse compressor is operated with a phase-modulated RF pulse to achieve a flat-top pulse at the output. The achieved stability using low-level RF based measurements is shown in Fig. 10. The stability is around 3.5 mK (rms) and this could be achieved even with temperature changes of  $\pm 0.5$ K in the supply water line.

After a larger change in the RF power level of the pulse compressor, it currently takes around 5 minutes for the regulation loop to reach steady-state again. We are investigating options to further increase the speed of the regulation circuit.

## SUMMARY AND OUTLOOK

Important achievements for the realization of the C-band accelerator have been made. The performance of the main RF components has been successfully demonstrated. An important milestone now is the assembly and test of a complete C-band module. Preparations for this are already on their way, and it is planned to have the first complete module operational in our test stand beginning of 2014. A second major milestone that has to be taken next year is the characterization and testing of the two prototype modulators that have been ordered.

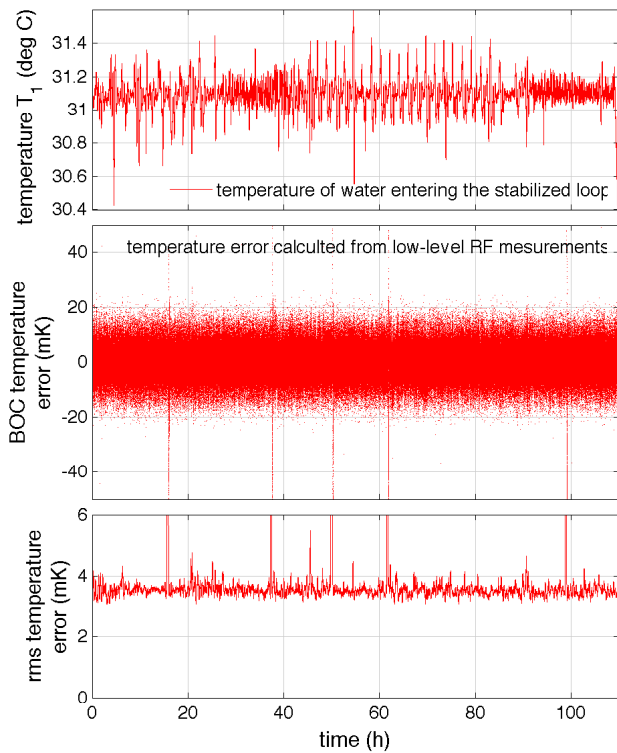


Figure 10: First measurement results with the prototype temperature stabilization system for the pulse compressor. Top: temperature  $T_1$  in the supply line. Center: temperature error calculated from low-level RF measurements. Bottom: rms temperature error of the pulse compressor.

## REFERENCES

- [1] “SwissFEL Conceptual Design Report,” PSI report 10-04, Paul Scherrer Institut, Villigen-PSI, Switzerland, 2010.
- [2] S. Sanfilippo et al., “Design and magnetic performance of small aperture prototype quadrupoles for the SwissFEL at the Paul Scherrer Institut,” MT-23 Conference, Boston, USA, 2013.
- [3] I. V. Syratchev, “The progress of X-band ‘open’ cavity RF pulse compression systems, EPAC 1994 Conference, London, England, 1994.
- [4] R. Zennaro et al., “C-band RF pulse compressor for SwissFEL,” IPAC 2013 Conference, Shanghai, China, 2013.
- [5] R. Zennaro et al., “C-band accelerator structure development and tests for the SwissFEL,” LINAC 2012 Conference, Tel-Aviv, Israel, 2012.
- [6] U. Ellenberger et al., “Status of the manufacturing process for the SwissFEL C-band accelerating structures,” FEL 2013 Conference, New York City, USA, 2013.